A transplant experiment helps identify the genetic basis of adaptation in *Timema* stick insects

Romain Villoutreix[1], Clarissa Ferreira de Carvalho[2], Zachariah Gompert[3], Thomas L. Parchman[4], Jeffrey L. Feder[5] and Patrik Nosil[1].

[1] CEFE, Univ Montpellier, CNRS, EPHE, IRD, Univ Paul Valéry Montpellier 3, Montpellier, France

[2] Universidade Federal de São Paulo (UNIFESP), São Paulo, Brazil

[3] Department of Biology, Utah State University, Logan, UT, USA

[4] Department of Biology, University of Reno, Reno, NV, USA

[5] Department of Biological Sciences, University of Notre Dame, Notre Dame, IN, USA

Corresponding authors: Patrik Nosil (patrik.nosil@cefe.cnrs.fr) and Romain Villoutreix (romain.villoutreix@gmail.com)

Running title: Bottom up genetic approach for adaptation in *Timema* stick insects

Keywords: epistasis, survival, genetic mapping, unmeasured traits, inversion, supergene

Abstract: 200 words max.

Identifying the genetic basis of adaptation is a central goal of evolutionary biology. However, identifying genes and mutations affecting fitness remains challenging because a large number of traits and variants can influence fitness and selected phenotypes can be difficult to know *a priori*, complicating top down genetic approaches for trait mapping that involve crosses or genome-wide-association studies. In such cases, bottom up genetic approaches, where one maps fitness directly and attempts to infer the traits involved afterward, are possible. Here, we re-analyse data from a field transplant experiment involving *Timema* stick insects, where five physically clustered SNPs associated with cryptic body colouration were shown to interact to affect survival. Our analyses here cover a larger genomic region than past work and revealed a previously unidentified locus as associated with survival. This locus resides near a gene, *Punch (Pu),* involved in pteridine pigments production, implying that it could be associated with an unmeasured colouration trait. However, by combining previous and newly obtained phenotypic data, we show that this trait is not eye or body colour related. We discuss the implications of our results for the discovery of traits, genes, and mutations associated with fitness in other systems, as well as for supergene evolution.

Background

The identification of adaptive mutations is a long-standing goal of evolutionary biology. This goal is important because such mutations represent the ultimate source for evolutionary change and affect the dynamics of evolution. In this regard, theory predicts that the rate and dynamics of adaptation are affected by properties of selected mutations, particularly their effect sizes, and pleiotropic and epistatic effects [1-4]. Specifically, in the absence of gene flow, mutations fixed by natural selection as populations adapt to constant selection pressures through time are expected to have exponentially smaller effect [3], and display intermediate levels of pleiotropy and epistasis [4]. The fixation of mutations with high levels of pleiotropy or epistasis might constraint adaptation and prevent a population from reaching its fitness optimum. Recent work has also explored how gene flow affects these predictions [5-7]. A characterization of many selected mutations is thus necessary to test the expectations of theory and constitutes an important step towards predict evolutionary outcomes in nature [8].

With recent advances in sequencing technologies, genes associated with selected traits have been identified in many systems, with causal mutations even being identified in some systems. Examples include genes and mutations affecting coat colour in deer mice *Peromyscus manuculatus* (*Agouti*; Δ Ser mutation) [8], defensive body armour in the threespined stickleback *Gasterosteus aculeatus* (*Eda*) [9], and flowering time in the mouse-ear cress *Arabidopsis thalina* (*Frigida*; multiple mutations) [10, 11]. Despite these discoveries, identifying genes and mutations underlying adaptation remains challenging in most systems.

A common approach to identify such genes and mutations, the top down genetic approach, begins with the identification of a selected trait, followed by dissection of its genetic basis, usually through crosses or genome wide association mapping (GWA, hereafter). Verifying the causal effects of genes and mutations on selected traits can then be accomplished through functional genetics (*e.g.*,

using Crispr-cas 9 or any other molecular manipulative tool) [12]. While useful, application of top down genetic approaches to many systems is challenging because the traits associated with fitness variation are not known or are difficult to detect. For example, in the fruit fly *Drosophila melanogaster* and the mosquito *Anopheles gambiae*, adaptation to environmental clines can involves behavioural, physiological, and phenological traits that cannot be directly observed and that require time consuming or specific methodologies to measure [13-15]. But because adaptation is expected to involve multiple traits, identifying all the traits associated with fitness is still challenging even in systems where a subset of traits is known to be associated with fitness variation [16]. To circumvent the problems associated with a top down strategy, another approach, the bottom up genetic approach [12], begins by using genome scans of natural populations to detect associations between genes and mutations with environmental variables [17, 18]. Following this initial step, the traits associated with these genes and mutations can then be identified through analysis of the molecular function of these genes and mutations, or through functional genetics by knocking out these genes or mutations and looking at resulting phenotypic changes [19].

While most studies employing a bottom up strategy start with genome scans of natural populations [17, 18], it is also possible to initiate such an approach with a manipulative field experiment. In this case, rather than surveying different populations to detect genetically diverged regions and genes in the genome, individuals from one environment are transplanted to another environment to identify loci displaying statistically significant changes between initial source and surviving transplant samples. Here, our initial analysis aims to identify associations between genes (and mutations) and the inclusive phenotype of survival or fitness, rather than correlations with particular environmental variables. One advantage of such an experimental approach is that it may be less susceptible to spurious associations than genome scans, in particular, when the natural populations being surveyed are geographically or demographically structured [17]. Examples of such experiments have now

been carried out in the deer mice *P. manuculatus*, the threespined stickleback *G. aculeatus*, *Rhagoletis* flies, *Timema* stick insects and *A. thaliana* [8, 20-23].

One important consideration potentially complicating the analysis of transplant experiments is that, depending on the selection regime experienced by the individuals, genes (and mutations) may often interact with each other to affect fitness (*i.e.*, epistasis), even if they have additive effects on selected traits (Fig. 1A) [24]. Indeed, for non-linear selection regimes (*e.g.* stabilizing selection, disruptive selection), or selection acting on trait combinations (*e.g.*, correlational selection), epistasis for fitness is expected. This is because under such selection regimes the fitness effects of a mutation that additively increases a trait value (*e.g.*, body length) will depend on whether the mutation occurs in a genetic background where it moves the phenotype closer to or further from a fitness peak (Fig. 1A). In other words, the same mutation can have different (sometimes opposite) effects on fitness depending on the genetic background it resides in (Fig. 1A). But detecting fitness epistasis is computationally challenging. For example, testing for interactions across all possible pairwise combinations for 1 million single nucleotide polymorphisms (SNPs hereafter) requires assessing a total of 499,999.5 million interactions ($C^2_{1,000,000}$). One method developed to overcome this problem, implemented in the software LT-MAPIT [25, 26], does not focus on identifying significant interactions between pairs of SNPs but rather quantifies interaction effects between a given SNP and all other SNPs included in the analysis (termed marginal epistasis). LT-MAPIT thus provides a single test of marginal epistasis per SNP, and drastically reduces the computational burden associated with epistasis analysis [25, 26].

In the present study, we use a manipulative field experiment to identify putatively selected genes in *Timema* stick insects. Specifically, we re-analyse survival data from a previous mark-release-and-recapture transplant experiment in *Timema chumash* stick insects [22], employing LT-MAPIT to determine if we may have missed loci contributing to fitness due to the focus of previous work on a

single narrow genetic region controlling body cryptic colouration [22]. *Timema* stick insects are a genus of wingless herbivorous insects that rely on cryptic body colouration to escape visual predators such as birds and lizards [27, 28]. In many *Timema* species, individuals exist with green or grey/brown (*i.e.* melanistic) body colouration, making them respectively more camouflaged on the leaves or stems of their host-plants [27-29]. In the transplant experiment, marked *T. chumash* were moved from a source population on Mountain Mahogany (*Cercocarpus*) to a combination of two host-plant species (*Adenostoma* and *Ceanothus*) that generated correlational selection on cryptic body colouration, favouring very green or very brown individuals, and selecting against intermediate body colouration. Before release, a single leg was dissected from all the experimental individuals in order to genotype them at tens of thousands of markers across their genomes. In past work, five SNPs in close proximity to each other (in a ~ 1 megabase pair genomic region; referred to as the indel locus hereafter; see below for details) on linkage group eight (LG8 hereafter) were found to be associated with cryptic body colouration and to interact with each other to explain survival in the transplant experiment. Whether additional loci outside of the indel locus affect survival was not tested and is thus our focus here.

There are *a priori* reasons to suspect that such loci may exist outside of the indel locus. In several species of the genus (*i.e. T. californicum, T. cristinae*, *T. landelsensis*, *T. petita* and, *T. poppensis*) the genomic region harbouring the five aforementioned body colouration SNPs is deleted in green haplotypes but present in the brown haplotype [29]. Interestingly, this deletion is associated with a ~10.5 megabase pair inversion (referred as the *Mel-Stripe* locus hereafter) in *T. cristinae* [22, 29], raising the possibility that genes controlling variation of undetected selected traits reside within the *Mel-Stripe* locus but away from the indel locus (Fig. 1.B). If so, then this finding would inform different non-exclusive hypotheses for why inversions are selected for [30]. Indeed, inversions can either be selected for because of the advantage of a breakpoint mutation(s) [31, 32], or because they strongly reduce recombination between alleles at different genes they contain, thus helping maintain

143 favoured allelic combinations [30, 32, 33]. These mechanisms could also act in conjunction, as
144 might occur in *T. cristinae* [30].
145
146 To accomplish our goal we first performed a 'traditional' GWA mapping analysis (*i.e.*, not
147 accounting for epistatic effects) on survival using SNPs within the *Mel-Stripe* locus, which yielded
148 limited evidence for genetic associations with survival. We next tested for epistasis for survival
149 within the *Mel-Stripe* locus using LT-MAPIT and identified two loci associated with survival. One
150 of these loci was previously known, and is located within the indel locus and contains the gene
151 *Scarlet (st)* which we hypothesized to be associated with cryptic body colouration in *Timema* [29].
152 The other previously unidentified locus is away from the indel locus, and contains two interesting
153 genes, *Chitinase 5 (Cht5)* and *Punch (Pu)*. Chitinases have been associated with cold or heat stress
154 tolerance in several insect species [34, 35] suggesting that this locus could be associated with heat
155 tolerance in *Timema*. However, the most intriguing candidate, *Punch,* controls the first step of
156 pteridine pigment production and is associated with eye and body colouration in many insect
157 species [36-39]. This led us to hypothesize that this locus could be primarily associated with eye
158 colour variation in *T. chumash*. We therefore collected new data on eye colouration from
159 photographs taken of the individuals used in the transplant experiment and then performed
160 'traditional' GWA mapping for this trait. Eye colouration mapped to the indel locus and, as we show
161 below, eye colouration and cryptic body colouration are strongly genetically correlated in *T.*
162 *chumash*. No association was detected, however, between eye or body coloration and the region
163 containing and surrounding the gene *Punch*. Our combined results therefore appear to refute the
164 hypothesis that our measured colouration traits were the target of selection associated with the SNP
165 residing near *Punch* in the transplant experiment.
166
167 Nevertheless, our results indicate that at least one selected locus, whether *Punch*, *Chitinase 5* or
168 neither, likely resides within *Mel-Stripe*, away from the indel locus. We discuss the general

implications of this finding and how methods such as those employed here could facilitate the detection of traits, genes, and ultimately causal variants associated with fitness in the wild.

Methods

Transplant experiment with *T. chumash*:

Full details concerning the transplant experiment with *T. chumash* are described in a previous publication [22]. We provide a brief overview of the relevant information for the current study here. Over 700 insects were collected from a single natural population (Angeles National Forest, CA, HF5 34° 15.584′ N, 118° 6.254′ W), on the host plant Mountain Mahogany (*Cercocarpus sp.*) from which we selected 437 healthy adults for use in the transplant experiment. We gave all selected individuals a unique id number, photographed them, gave them an individual mark on the ventral side using Sharpie pens (*i.e.*, dots of different colour combinations) and released them back into the area they were collected from in one of two host-plant treatments (*i.e.*, different host plant species dominating the vegetation in this population, details below). Before release, we took a leg (*i.e.*, tissue sample) from each transplanted individual for DNA sequencing purposes. In the first treatment, we released 219 individuals onto isolated vegetation patches composed of intertwined plant individuals, one of each of two plant species (*Ceanothus sp*. and *Adenostoma sp.*; referred as AC treatment hereafter). In the second treatment we released 218 individuals onto an isolated Mountain Mahogany host plant (*Cercocarpus sp.*; referred as MM treatment hereafter). We recaptured surviving individuals ~72h after release. Past studies with similar experimental design have shown that dispersal of *Timema* across bare ground is essentially non-existent such that recapture is a good proxy for survival [40, 41].

For all analyses except for the GWA mapping of for body and eye colouration, we only used data from the AC treatment, as this is the only treatment where past work found evidence for correlational selection on cryptic body colouration [22]; thus epistasis for fitness is only strongly

expected in the AC treatment. However, eye and body colouration can be measured independently from treatment. Thus, for GWA on eye and body colouration, we used data both from the AC and MM treatments.

We here re-analyse published genomic data from the transplanted individuals. These data are published and were generated in the aforementioned past study [22] using a standard genotyping-by-sequencing approach with two restriction enzymes (*i.e.* ddRAD) [42]. Details concerning filtering, read alignment and variant calling are described in past work [22]. For the current study we generated new data on eye colouration and conducted novel analyses of the genetic basis of this trait.

GWA for survival within the *Mel-Stripe* locus using GEMMA

We first quantified associations between genotypes at bi-allelic SNPs (we also used only bi-allelic SNPs for all subsequent analyses) within the *Mel-Stripe* locus and survival using a mapping approach that does not explicitly consider epistasis, implemented in the software GEMMA [43, 44]. For these analyses, we excluded SNPs with a minor allele frequency < 0.01 and fit a probit Bayesian sparse linear mixed model. We set 5 MCMC chains with the following parameters: a burnin of 1 million iterations, a run of 3 million iterations, and a record time of every hundred iterations. Following past work, we calculated posterior probabilities from the combined output of the five MCMC chains [22, 27, 29].

Estimating marginal epistasis for survival within the *Mel-Stripe* locus using LT-MAPIT

We tested for SNPs that exhibit epistatic effects on survival (*i.e.*, interact with other SNPs) using the software LT-MAPIT [25, 26]. Briefly, this method detects SNPs with non-zero marginal epistatic effects defined as the combined pairwise interaction effects between a given focal SNP and all other SNPs included in the same analysis [25]. LT-MAPIT was originally designed for case-control

studies and is therefore an appropriate method to use to analyse our binary survival data. We set the disease prevalence parameter in LT-MAPIT as the survival empirically observed in the transplant experiment (51 recaptured individuals / 219 released individuals = 23.28%). We conducted additional analyses that consider individual pairs of SNPs using different methods, as described below.

Finding *Drosophila melanogaster* homologs for genes in the vicinity of LT-MAPIT outlier 2

We attempted to identify potential traits associated with LT-MAPIT outlier 2 by selecting all predicted genes located within 200 kilo base pairs (kb) of this SNP and looking for their homologs (if any) in the *Drosophila melanogaster* genome. We then searched for described phenotypic effects of these homologs in *D. melanogaster* and other insects, which allowed us to hypothesize what trait(s) might be associated with these genes in *Timema*. Specifically, we identified *D. melanogaster* homologs for our predicted genes with the blastn function on the NCBI website (https://blast.ncbi.nlm.nih.gov/Blast.cgi#) [45] using only the coding sequence of our predicted genes as a query and restricting our search to *D. melanogaster* sequences only (taxid:7227). We obtained the coding sequences of our predicted genes of interest from our 1.3c2 *T. cristinae* reference genome and annotation [29, 46] using the gestfasta function from the bedtools software (bedtools version 2.28.0). If we successfully identified a homolog in *D. melanogaster* for our predicted genes of interest, we then looked for molecular function and phenotypic effects of the *D. melanogaster* homolog genes in flybase (https://flybase.org/) [37] and searched in the literature for phenotypic effects of these homolog genes in other insects.

Eye colouration measurements from photographs

Following past work where we measured body colouration from photographs of insects used in the transplant experiment [22], we corrected raw photographs (*i.e.* .NEF format) taken during the experiment for temperature set at 6150 °K in the software RawTherapee (version 5.8;

https://www.rawtherapee.com/) and exported them as JPEG images. We scored eye colouration from these JPEG images using ImageJ [47] (version 1.52r; https://imagej.nih.gov/ij/) circling the right eye (when not possible we measured the left eye) with the polygon tools and using the Color Histogram add-on (Sup. Fig. 1). Following past work, we measured the RGB colour channels (red, green and blue) and processed them following ref. [48] to obtain RG and GB estimates (the ratio of red over green and the ratio of green over blue, respectively) [22, 27, 29].

GWA mapping for eye and body colouration.

We conducted GWA mapping on the new eye colouration traits using GEMMA [43, 44] and also on body colouration traits to allow eventual estimation of the genetic correlation between eye and body colouration (details below). For this, we fit a Bayesian sparse linear mixed model using the same parameters described above for survival.

Estimating the number of unlinked genetic variants (*i.e.*, quantitative trait nucleotide, *QTN*) for eye colouration within the indel locus:

We followed past work to obtain the total number of genetic variants affecting eye colouration within the indel locus using our GEMMA models [29]. Briefly, GEMMA outputs a PIP value (*i.e.*, Posterior Inclusion Probability) for each SNP which corresponds to the proportion of recorded MCMC steps in which the SNP was found to have a measurable effect on the phenotype. PIP values are therefore bounded between 0 (the SNP was never found to have a measurable effect on the phenotype) and 1 (the SNP was found to always have a measurable effect on the phenotype). One can therefore estimate the number of causal variants affecting each trait in a genomic region by summing the PIPs for all SNPS in that region. For example, for a polygenic trait with recombination among loci, the one or few SNPs that best tag each causal variant are expected to consistently be associated with the trait across MCMC steps (*i.e.*, exhibit high PIP values). Thus, PIPs across such SNPs sum to an estimate of the number of total causal variants.

However, because of pleiotropy or close genetic proximity (*i.e.*, high linkage disequilibrium) some SNPs within the indel locus were found to be associated with both eye colouration traits (RG and GB), potentially inflating our estimate of variant number. We therefore corrected our estimate for the number of total causal variants affecting eye colouration within the indel locus with the following method. For each SNP within the indel locus, we summed their PIP values for both RG and GB. If this value was above one, we set it to one. We then summed these values over all SNPs within the indel locus. Our corrected estimate is certainly an under-estimation of the true number of variants within the indel locus, the real number of unlinked variants will be somewhere in between the corrected estimate and the uncorrected estimate.

Genetic correlation between eye and body colouration:

We estimated the genetic correlation between eye and body colouration using polygenic scores estimated with GEMMA's predict option [43, 44]. Specifically, for each trait we masked the phenotype of a quarter of the sampled individuals (*i.e.*, 109 individuals) and ran a Bayesian sparse linear mixed model GWA mapping model with one MCMC chain for the remaining individuals (the same parameters were used as for survival described above). We repeated this process four times for each trait, allowing us to get predicted phenotypic value (i.e., polygenic score) for each individual. The correlation between polygenic scores for eye and body colouration (*i.e.*, the genetic correlation) was estimated using Pearson's correlation coefficient.

Comparing the genetic bases of eye and body colouration:

To test if eye and body colouration might be controlled by similar genetic regions, we compared the lists of the most highly associated SNPs for each trait, between eye and body colouration traits (RG and GB). Specifically, because GEMMA analyses indicated that most traits were controlled by ~10

SNPs, we selected the 10 most-associated SNPs for each trait and looked for intersections between these lists (*i.e.*, SNPs present in both lists).

To test if the observed frequency of sharing/overlap of the most associated SNPs between eye and body colouration traits could arise by chance, we generated a distribution of overlap expected under random sampling. Specifically, we sampled 10 items from an ensemble with a number of elements (*i.e.*, cardinality) similar to the total number of input SNPs in our GEMMA analysis. We repeated this operation to obtain a second sample and recorded the number of items picked in both samples. We repeated these two operations a million times to obtain the expected distribution of shared elements in two samples under random sampling. We compared the observed number of shared SNPs to this null distribution to obtain a *P-value*.

Quantifying our ability to predict survival based on LT-MAPIT outlier SNPs:

We tested whether allowing for epistatic interactions between LT-MAPIT outlier SNPs and other SNPs within *Mel-Stripe* improved our ability to predict survival. To determine this, we fit binomial generalized linear models with Bayesian model averaging. Ten-fold cross-validation was used to assess predictive performance for the full model (with epistasis; model 1 – see below) and reduced model (without epistasis; model 2 – see below) while averaging predictions of survival over sub-models including different subsets of covariates. We fit these models using the bic.glm function in the R BMA package (BMA version 3.18.15) [49]. We assigned all covariates prior inclusion probabilities of 0.5 (i.e., equally likely to be in or left out of the model). For cross-validation, each observation was left out of one of the ten training sets. Specifically, we tested the following full (with epistasis) and reduced (without epistasis) models:

$$\text{Survival} = \text{intercept} + \text{outlier1} + \text{outlier2} + \text{PCA1} + \text{outlier1 x outlier2} + \text{outlier1 x PCA1} + \text{outlier2 x PCA1} + \text{err.} \quad \text{(model 1)}$$

Survival = intercept + outlier1 + outlier2 + PCA1 + err. (model 2)

Where intercept= a constant, outlier1= genotype estimate at the LT-MAPIT outlier SNP 1 (near the *st* gene), outlier2 = genotype estimate at the LT-MAPIT outlier SNP 2 (near the *GTP cyclohydrase I* gene), PCA1= individual value on the first axis from a PCA realized on all SNPs within the *Mel-Stripe* locus excluding the LT-MAPIT outlier SNPs, outlier1 x outlier2 = the interaction between the LT-MAPIT outlier SNPs, outlier1 x PCA1 = the interaction between the outlier1 SNP and the first axis from a PCA of all SNPs within the *Mel-Stripe* locus excluding both LT-MAPIT outliers SNPs, outlier2 x PCA1 = the interaction between the outlier 2 SNP and the first axis from a PCA of all SNPs within the *Mel-Stripe* locus excluding both LT-MAPIT outlier SNPs, err = the error term.

Estimation of recombination within the *Mel-Stripe* locus in *T. cristinae*:

To assess if recombination suppression varied in the *Mel-Stripe* locus in *T. cristinae* we estimated linkage disequilibrium in the genomic region surrounding and including it. Specifically, we reanalysed GBS data from 602 insects collected in 2013 from a single polymorphic population of *T. cristinae* (FHA; 34.52, -119.8) [27, 29]. Briefly, we extracted DNA from legs and generated genotypes at thousands of markers across the genome for these samples using a standard genotyping-by-sequencing approach with two restriction enzymes (*i.e.* ddRAD) [42]. Details concerning alignment, variant calling and filterning are described in past work [29]. The data set included 175,918 SNPs with 8,149 SNPs within the two LG8 scaffolds containing *Mel-Stripe* (702.1 and 128) or the scaffolds directly adjacent to these (2963 and 1845), which we focus on here (this focal region covers ~51 megabases including the ~10 megabase *Mel-Stripe* locus). We first estimated allele frequencies for the SNPs in this data set using an expectation-maximization algorithm that accounts for uncertainty in genotypes caused by sequence error and finite sequence coverage (Li, 2011). This was done with estpEM (version 0.1) with a tolerance threshold of 0.001

and 40 maximum iterations (Soria-Carrasco et al., 2014; Riesch et al., 2017; DRYAD https://doi.org/10.5061/dryad.nq67q). We then obtained empirical Bayesian estimates of genotypes as $g_{ij} = L(g_{ij}=0)\ (1-p_i)^2 + L(g_{ij}=1)\ 2\ p_i\ (1-p_i) + L(g_{ij}=2)\ p^2$, where g_{ij} is the genotype estimate (number of non-reference alleles) for SNP *i* and individual *j*, $L(\cdot)$ is the genotype likelihood from samtools/bcftools (as computed in [29]), and p_i is the non-reference allele frequency from estpEM. Lastly, we computed linkage disequilibrium for all pairs of SNPs in 100 kilobase windows along the four genome scaffolds considered here, which included all of the *Mel-Stripe* locus. LD was measured as the squared genotypic correlation for pairs of SNPs. We used the mean estimate of pairwise LD within each window as our summary of LD for that window. LD calculations were performed in R (version 4.0.2).

Data and script availability:

All data and scripts are archived in the following DRYAD repository: xxx. We conducted analyses, summarized the results and generated graphics with custom perl and R scripts [50] (perl version 5.16.3; R version 3.6.0 or 4.0.2).

Results

Association mapping for survival within the *Mel-Stripe* locus without epistasis:

We first tested for associations between SNPs within *Mel*-Stripe and survival (Fig. 2), using a multi-SNP approach that does not account for epistasis. As expected, because of the selective regime imposed by the transplant experiment for cryptic body colouration in the AC treatment (*i.e.*, disruptive/correlational selection for cryptic body colouration) [22], this approach explained little variation in survival (2% of variance explained; 0-23% as 95 % equal-tail probability intervals). All SNPs exhibited appreciable posterior inclusion probabilities (PIP), but we did not detect individual SNPs with exceptionally high PIPs (Fig. 2). This pattern is most likely an artefact of the MCMC approach when using a relatively small number of SNPs and when strong associations do not exist

for any SNP with the trait studied. In other words, SNPs are largely redundant (*i.e.*, they each explain little variation) and have a high prior probability to be randomly picked by the MCMC chain over 3 million iterations, leading to somewhat inflated PIPs for all SNPs examined [43, 44].

Epistasis for survival within the *Mel-Stripe* locus:

We next tested for evidence of epistasis between SNPs within *Mel-Stripe* associated with survival, using LT-MAPIT, a method that tests for epistasis between a particular focal SNP and the remaining input SNPs (here all other SNPs within the *Mel-Stripe* locus; Fig. 3). This method quantifies interaction effects between the focal SNP and a variable summarizing the remaining genetic variation within *Mel-Stripe* (*i.e.*, marginal epistasis), in a fashion similar to a principle component axis. From this analysis we identified five SNPs with nominally significant marginal epistasis (*p-value* <= 0.05), two of which were clear outliers with particularly strong evidence for epistasis (Fig. 3). One of these outlier SNPs (outlier 1, hereafter) is located within the indel locus, while the other is located within the *Mel-Stripe* locus but away from the indel locus (outlier 2 hereafter; Fig. 3).

Potential function of the two LT-MAPIT outlier SNPs:

We next examined the predicted genes in physical proximity (*i.e.*, located within 200 kilobase pair) of the two LT-MAPIT outlier SNPs in order to identify candidate genes and traits potentially associated with these two loci (Table 1, and Sup. Table 1 & 2).

Outlier 1 is located within the indel locus and situated ~56kb from the *st* gene (predicted gene g6239), coding the protein scarlet. The *st* gene is known to affect different aspects of colouration in several insect species [51-53], and was one of the prime candidate genes for cryptic body colouration identified in past *Timema* work [22, 29].

Outlier 2 is not within the indel locus, being ~3.7 megabase pair away from it. There are several predicted genes with various molecular functions, including a chitinase II, a *GTP cyclohydrase I* enzyme, a TORC2 component, and the target of rapamycin complex 2 in proximity to LT-MAPIT outlier 2 (Table 1, and Sup. Table 2). The predicted gene coding for a chitinase II (g6060) is an intriguing candidate. This gene is located ~19 kilobase pair away from LT-MAPIT outlier 2, is homologous to the *Chitinase 5 (Cht5)* gene in *Drosophila melanogaster*, and codes for an enzyme involved in the formation of chitin-based extracellular matrix at barrier tissues [37]. Interestingly, enzymes of the same family have been associated with cold or heat tolerance in insects [34, 35], leading us to hypothesize that LT-MAPIT outlier 2 could be associated with heat tolerance in *Timema*. Further experiments are yet needed to test this hypothesis. However, the most intriguing candidate gene (predicted gene g6064) is located ~118 kilobase pair away from outlier 2 and[54] is homologous to the *Punch (Pu)* gene in *Drosophila melanogaster* (Table 1). This gene codes a GTP cyclohydrase I enzyme, which is involved in the first step of the production of pteridine pigment synthesis in *D. melanogaster* and other insects, and is associated with eye and body colouration in multiple insect species [36-39, 54][36, 39]. This led us to hypothesize that this SNP could also be associated with *T. chumash* eye colouration, a trait we observed to be quite variable but which is previously unstudied in this species (Sup. Fig. 2). We test this latter hypothesis in the following section.

Genetic basis of eye colouration in *T. chumash*:

To test our eye colouration hypothesis, we measured eye colouration in all experimental individuals from photographs and conducted a GWA mapping analysis for this trait. Here, because we did not have a strong *a priori* expectation concerning the genetic architecture of eye colouration, we did not restrict our analysis to the *Mel-Stripe* locus but instead tested for associations across the entire genome. Our models revealed that eye colouration is controlled by a modest number of SNPs (eye-RG: 6 SNPs with detectable effects, range 2 to 19 for 95 % equal-tail probability interval; eye-GB: 6 SNPs with detectable effects, range 3 to 16 for 95 % equal-tail probability interval). Genetic

variation for loci with measurable phenotypic effects explained a substantial amount of phenotypic variation in our models (obtained by multiplying the PVE and PGE hyper-parameters; eye-RG: 51% range 31% to 76% for 95 % equal-tail probability interval; eye-GB: 49%, range 32% to 68% for 95 % equal-tail probability interval). Our results indicate that SNPs associated with eye colouration are located on different chromosomes (Sup. Fig 3 and Sup. Fig 4), however, SNPs within the indel locus showed the highest associations with eye colouration traits (Fig. 4). We estimated that the indel locus contained a maximum of four QTN for eye colouration traits (two QTN each, for RG and GB, but these QTN overlapped between colouration traits; the true number of independent QTN is thus likely somewhere between two and four). However, the region surrounding *Punch* did not display an association with eye colouration traits suggesting that, contrary to our hypothesis, LT-MAPIT outlier SNP 2 is not associated with eye colouration.

Test for shared genetic basis of body and eye colouration:

Given that body and eye colourations are at least in part controlled by the indel locus, we tested if eye and body colouration share similar genetic bases. Indeed, this is expected given that we found here that body and eye colourations are strongly phenotypically correlated (Pearson's correlation coefficients on phenotypic values: RG=0.87, *P-value* < $2.2e^{-16}$, GB=0.77, *P-value* < $2.2\ e^{-16}$; Fig. 5). Moreover, explicit estimation of the genetic correlation between eye and body colouration traits revealed strong genetic correlations (Pearson's correlation coefficients on polygenic scores: RG=0.92, *P-value* < $2.2e^{-16}$, GB=0.88, *P-value* < $2.2e^{-16}$; Fig. 5).

Our results indicate that some SNPs were found to be most associated with both eye and body colouration and that this number of shared SNPs is greater than what can be expected by chance (eye and body RG: 5 shared SNPs, *P-value* < $1x10^{-6}$; eye and body GB: 4 shared SNPs, *P-value* < $1x10^{-6}$). This suggests that genes near these SNPs have pleiotropic effects on both body and eye

colouration, or that multiple genes independently controlling body and eye colouration are in close physical proximity.

Predicting survival based on LT-MAPIT outlier SNPs:

Finally, we asked whether allowing for epistatic interactions between LT-MAPIT outlier SNPs and the rest of genetic variation within *Mel-stripe* improved our ability to predict survival relative to a model without epistasis.

When fit with all of the observations, we found that the sub-models predicting the best survival for the full (with epistasis) and reduced (without epistasis) models were those that included only an intercept term. These intercept-only sub-models had posterior probabilities of 0.593 and 0.781 for the full and reduced models, respectively. Moreover, posterior probabilities that individual covariates (additive or epistatic effects) affected survival were ~10% or less (Table 1). Using all of the data for model fitting and prediction, correlations between survival and predicted survival were slightly higher for the model with epistasis (r = 0.125, 95% CI = -0.007 – 0.254, P = 0.064) than for the model without epistasis (r = 0.092, 95% CI = -0.041 – 0.222, P = 0.175). However, in both cases a correlation of 0 could not be strictly rejected. Moreover, when using predictions from cross-validation, which specifically measures predictive performance and avoids over-fitting, we failed to predict survival. Indeed, we observed negative correlations between predicted and observed survival (full model, r = -0.179, 95% CI = -0.305 - -0.048, P = 0.0078; reduced model, r = -0.216, 95% CI = -0.339 - -0.086, P = 0.0013). It therefore appears that we have little ability to actually predict survival with or without epistatic terms in our model, although we were able to map a portion of its genetic basis. This is perhaps not surprising for a complex and integrative trait like survival, but forms a major point of our discussion below.

Discussion

Our results show that a bottom up approach based on a manipulative field experiment was useful for identifying candidate genes not previously shown to be associated with fitness in *Timema* stick insects. In particular, by mapping survival in a transplant experiment with *T. chumash* and explicitly taking epistasis into account, we detected a genomic region in the *Mel*-Stripe locus on LG8 not previously known to be associated with survival in *Timema*. Despite collecting new eye colouration data and trying to determine the nature of the phenotype controlled by this region, we were not able to identify genotypic variation influencing this trait. Although the functional annotation of a gene, *Punch*, in proximity to the SNP associated with survival suggested a possible association with eye colouration, we found no evidence for this in a subsequent GWA analysis of the trait. Thus, the phenotype encoded by this region might be related to an aspect of colouration that we did not measure in the study. Alternatively, the presence of the *Chitinase* 5 gene in this region suggest that it could be associated with heat tolerance in *Timema*, as chitinase genes are associated with cold or heat adaption in other insect species [34, 35]. We have evidence that melanistic morphs in *T. cristinae* are more sensitive to heat stress [46], and we speculate that this locus could interact with colour loci in *Timema* to allow better heat tolerance in melanistic individuals. Further experiments involving GWA of heat tolerance in a population of *T. chumash* with body colour variation are necessary to test this hypothesis. Another way to potentially identify the selected trait(s) associated with this region could involve genetic manipulations of these two candidate genes using functional tools such as CRISPR/Cas9 and RNAi and looking for any resulting phenotypic changes in transformed individuals [55].

One seemingly counterintuitive aspect of our results is that despite finding evidence that selection is likely acting on a previously unknown locus in the *Mel-Stripe* locus and one locus in the indel locus in *T. chumash*, inclusion of these two LT-MAPIT outlier SNPs, even when including their epistatic effects with other genes across these regions, did not have notable consequences for increasing the predicted survival of insects in the transplant experiment. In this regard, it is important to appreciate

that the deterministic component of survival generally represents the sum total of many traits encoded by many genes, often of relatively small effect size, collectively affecting fitness. Thus, while a particular variant may show a significant association with fitness, this does not mean that the mutation will necessarily make a substantial contribution to predicting whether an individual possessing the mutation will survive, given the many other loci and phenotypes are likely involved.

Our results therefore highlight the utility of manipulative experiments for identifying potential genes under selection, but also the challenges that can remain in verifying the specific loci, mutations, and phenotypes involved. Nevertheless, we propose that the bottom up approach employed here could be useful for the study of adaptation in many organisms. Indeed, a similar manipulative approach was used in the threespine stickleback *G. aculeatus* where marine fishes were transplanted into four experimental fresh water ponds and phenotypic and genetic evolution were tracked for the two subsequent generations [16, 20]. This experiment confirmed that reduced defensive body armour is selected for in the fresh-water environment, along with its underlying gene (*Eda*) [16, 20]. Interestingly, this experiment also confirmed that defensive body armour is likely not the sole trait controlled by the *Eda* gene [16], which also appears to influence four other selected traits including lateral plate count, neuromast number, neuromast pattern and, to some extent, body shape [56]. All of these traits are genetically correlated because of both pleiotropy and close physical linkage of mutations within the *Eda* gene region [56]. The methods employed in the threespine stickleback studies are well suited for traits experiencing directional selection. The methods we employed in this study are well tailored for traits experiencing non-linear selection (*e.g.* stabilizing or disruptive selection), or selection acting in concert on multiple traits (*e.g.* correlational selection) and therefore constitute a useful addition for the identification of adaptive genes and mutations in natural populations. These methods will be especially useful for the study of balanced polymorphisms, where selective pressures promote the coexistence of two or more alleles

via stabilising selection [57, 58]. This excludes neutral polymorphisms, or transient polymorphisms where one form is in the process of replacing another within the population [58].

Our results also provide insight on the evolution of genetic architecture. Specifically, we here provide the first evidence in *Timema* for a selective locus residing within the *Mel-Stripe* locus but away from the indel locus (Fig. 1). This finding sheds new light on the chromosomal inversion associated with colour morphs in *T. cristinae* [29, 59], which spans the *Mel-Stripe* locus (and suppress recombination evenly throughout this locus; Fig. S5), and even more generally, on regions of suppressed recombination on LG8 that extend beyond the indel locus (these regions of suppressed recombination may be widespread in *Timema*, although direct evidence for inversions in other *Timema* species awaits further data [29]). In *T. cristinae* the selective advantage of the *Mel-stripe* inversion may involve the combination of the deletion at one breakpoint affecting body colouration [29], and another locus (potentially *Punch*) within the inversion. If true, then two possible scenarios could account for the evolution of this inversion in *T. cristinae*. In the first scenario, the inversion might have initially been selected because of an adaptive breakpoint mutation, with genetic variation at the second locus evolving afterward. Such a 'breakpoint first' scenario is conceptually similar to models describing the accumulation of genetic incompatibilities in inversions after their formation proposed by Navarro and Barton in a model of parapatric divergence [60]. In the second scenario, the inversion may have simultaneously trapped pre-existing genetic variation within the *Mel-Stripe* locus with a newly generated adaptive breakpoint mutation(s), which share some conceptual similarities with the local adaptation scenario for the spread of inversions proposed by Kirkpatrick and Barton [61], and modified by Feder and colleagues to allow for allopatry and secondary contact [62]. These scenarios expand upon the conditions under which inversions may contribute to adaptation, the most well-known being the ability for inversions to spread because their effects on suppressing recombination and maintaining favourable allelic combinations (*i.e.*, keep such combinations intact [61]). Distinguishing between

the two scenarios noted above in *Timema* will be important to evaluate the contribution and order of evolution of mutations and genome rearrangement in adaptation. Future work in *T. cristinae* should allow such characterisation, specifically by independently dating the inversion and the adaptive genetic variation it contains [30].

In conclusion, our study highlights that manipulative experiments can be useful to identify adaptive genes and mutations, especially when traits associated with fitness variation are not known. The methods we employed, because they explicitly consider epistasis, are particularly suited for the study of non-linear forms of selection (e.g., balanced polymorphisms) which may be widespread in nature. Our results also highlight several challenges associated with elucidating the genetic basis of adaptation, and integrative traits like fitness. With creative use of modern sequencing technologies, analytical advances, natural history information, and experiments, we believe the field is poised to continue to tackle these challenges.

Acknowledgements

RV, PN and ZG conceived and preformed the experiment. RV, CFdC, TP and PN gathered data from the transplant experiment. RV, PN and ZG analysed the results of the experiment with the help of all authors. RV and PN wrote the manuscript with the help of all authors. This study is part of a project that has received funding from the European Research Council (ERC) under the European Union's Horizon 2020 research and innovation programme (Grant agreement No. 770826 EE-Dynamics). RV and PN were supported by the aforementioned ERC grant (Grant agreement No. 770826 EE-Dynamics). CFdC was supported by the Fundação de Amparo à Pesquisa do Estado de São Paulo (2020/07556-8; Dimensions US-BIOTA-Sao Paulo 18/03428-5). JF was supported by grants from the National Science Foundation and the United States Department of Agriculture. ZG was supported by the US NSF (DEB 1638768). TP funding? This work greatly benefited from the use of the University of Utah CHPC cluster and we are thankful to the team maintaining and running this

cluster. We are thankful to Cherie Topper and Holly Sherwin for providing us accommodation during our repeated field seasons in California and for their enthusiastic support of our research program.

584 **Tables.**

585 [37][37][37][37]

586

Tcri	Dmel	Molecular function in Dmel	Effects in Dmel	Effects in other insects	Hypothesized effects in *Timema*
g6060	Chitinase 5 (Cht5)	Encodes an enzyme involved in the formation of chitin-based extracellular matrix at barrier tissues [37]	lethality [37]	cold/heat tolerance [34, 35]	heat tolerance
g6064	Punch (Pu)	Isoform B is required for eye pigment production, Isoform C may be required for normal embryonic development and segment pattern formation [37]	abnormal eye colouration, lethality, sterility [37]	eye and body colouration [39]	eye colouration
g6057	-	-	-	-	-
g6058	-	-	-	-	-
g6068	Kramer (Kmr)	Predicted to enable phosphatidylinositol biphosphate binding activity. Involved in regulation of establishment of planar polarity. [37]	lethality, abnormal planar polarity [37]	-	-

587

588 *Table 1. Hypothesized function for predicted genes located less than 200 kb way from LT-MAPIT outlier SNP 2*. Only genes with identified molecular
589 functions were considered here. Tcri: gene number in *T. cristinae* reference genome 1.3c2, Dmel: homologue in *Drosophila melanogaster*, Molecular
590 function in Dmel: molecular function of this gene in *D. melanogaster*, Effets in Dmel: observed phenotypic effects of this gene in *D. melanogaster*,
591 Effets in other insects: observed phenotypic effects of this gene or genes in the same family in other insects species, Hypothesized effects in *Timema*:
592 hypothesized phenotypic effects of this gene in *Timema*.

	Full model (with epistasis)		**Reduced model (without epistasis)**	
Covariate	**Prob != 0**	Estimate (SD)	**Prob != 0**	**Estimate (SD)**
PCA1	0.051	0.006 (0.048)	0.067	0.008 (0.055)
Outlier 1	0.075	0.012 (0.055)	0.099	0.015 (0.063)
Outlier 2	0.040	-0.001 (0.032)	0.053	-0.001 (0.037)
Outlier 1*outlier 2	0.070	0.018 (0.092)		
Outlier 1* PCA1	0.052	0.017 (0.121)		
Outlier 2 * PCA1	0.118	-0.037 (0.125)		

Table 2. Summary of parameter estimates from Bayesian model averaging of sub-models with (full model) or without (reduced model) epistasis that were used to predict survival. The covariates included in each model are listed, and the posterior probability that each associated regression parameter is non-zero (Prob != 0) is given along with the model-averaged point estimate (posterior mean) and posterior standard deviation for each coefficient. Outlier1= genotype probability at the LT-MAPIT outlier SNP 1 (near the *st* gene); Outlier2 = genotype probability at the LT-MAPIT outlier SNP 2 (near the *GTP cyclohydrase I* gene); PCA1= individual value on the first axis from a PCA realized on all SNPs within the *Mel-Stripe* locus excluding the LT-MAPIT outlier SNPs; Outlier1 * outlier2 = the interaction between the LT-MAPIT outlier SNPs; Outlier1 * PCA1 = the interaction between the outlier1 SNP and the first axis from a PCA realized on all SNPs within the *Mel-Stripe* locus excluding both LT-MAPIT outliers SNPs; Outlier2 * PCA1 = the interaction between the outlier 2 SNP and the first axis from a PCA realized on all SNPs within the *Mel-Stripe* locus excluding both LT-MAPIT outlier SNPs.

Figures.

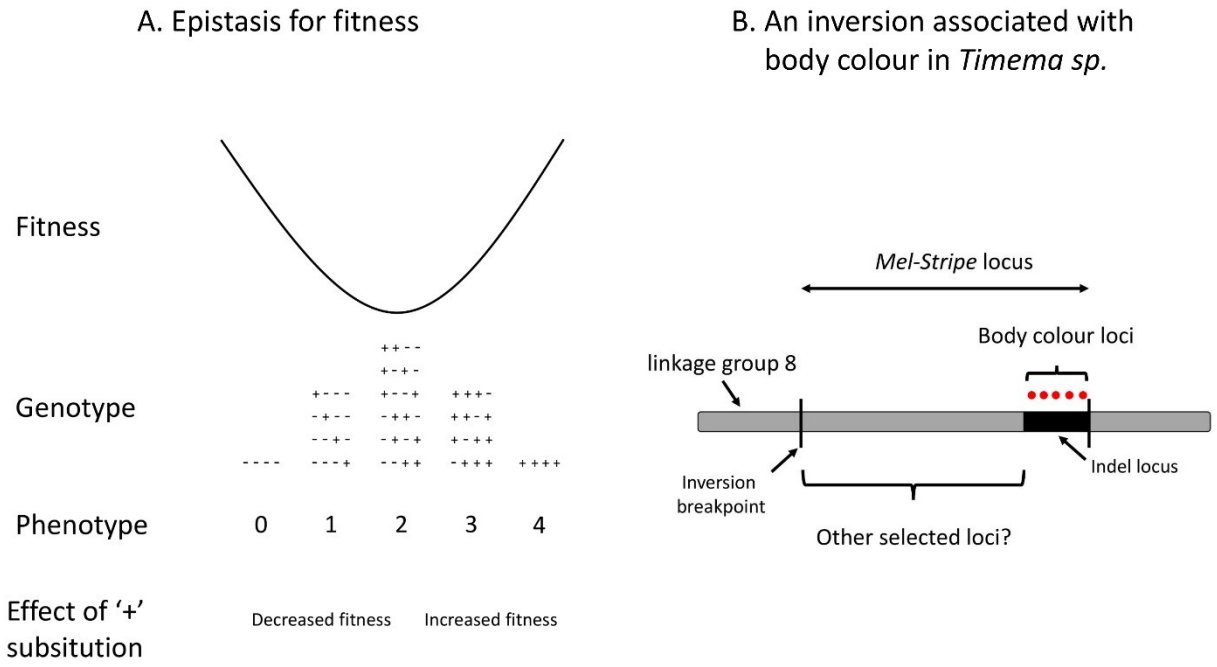

Figure 1. **A**: Disruptive selection on a trait with an additive genetic basis generates epistasis for fitness. The trait is controlled by four genes, each gene having two alleles (denoted here as plus and minuses). For simplicity, we represented the situation for a haploid organism, but the same property would emerge for diploid organisms. The pluses and minuses represent the relative effects of alleles on the trait (*i.e.* plus increase the trait value and minuses decrease it). The fitness effect of a particular allele depends on the alleles present at other genes (*i.e.*, epistasis for fitness). For example, a plus allele is detrimental when accompanied by three minus alleles because it will move the mean phenotype towards a larger trait value, away from the extreme and associated with lower fitness. In contrast, the same plus allele will be favoured when accompanied by at least two more plus alleles. Figure modified and redrawn from [24]. **B**: An inversion located on linkage group 8 is associated with body colour in *Timema cristinae* (*i.e.*, the *Mel-Stripe* locus depicted here). Body colour loci are deleted in *T. cristinae* green haplotypes (indel locus). The deletion is located in the vicinity of a breakpoint of the inversion. The existence of other loci associated with divergently selected traits within *Mel-Stripe*, but away from the indel locus, is yet to be tested and is the core objective of the current study. *Mel-Stripe* is estimated to have a length of at least 13.4 megabase pair, the indel locus ~1.4 megabase pair.

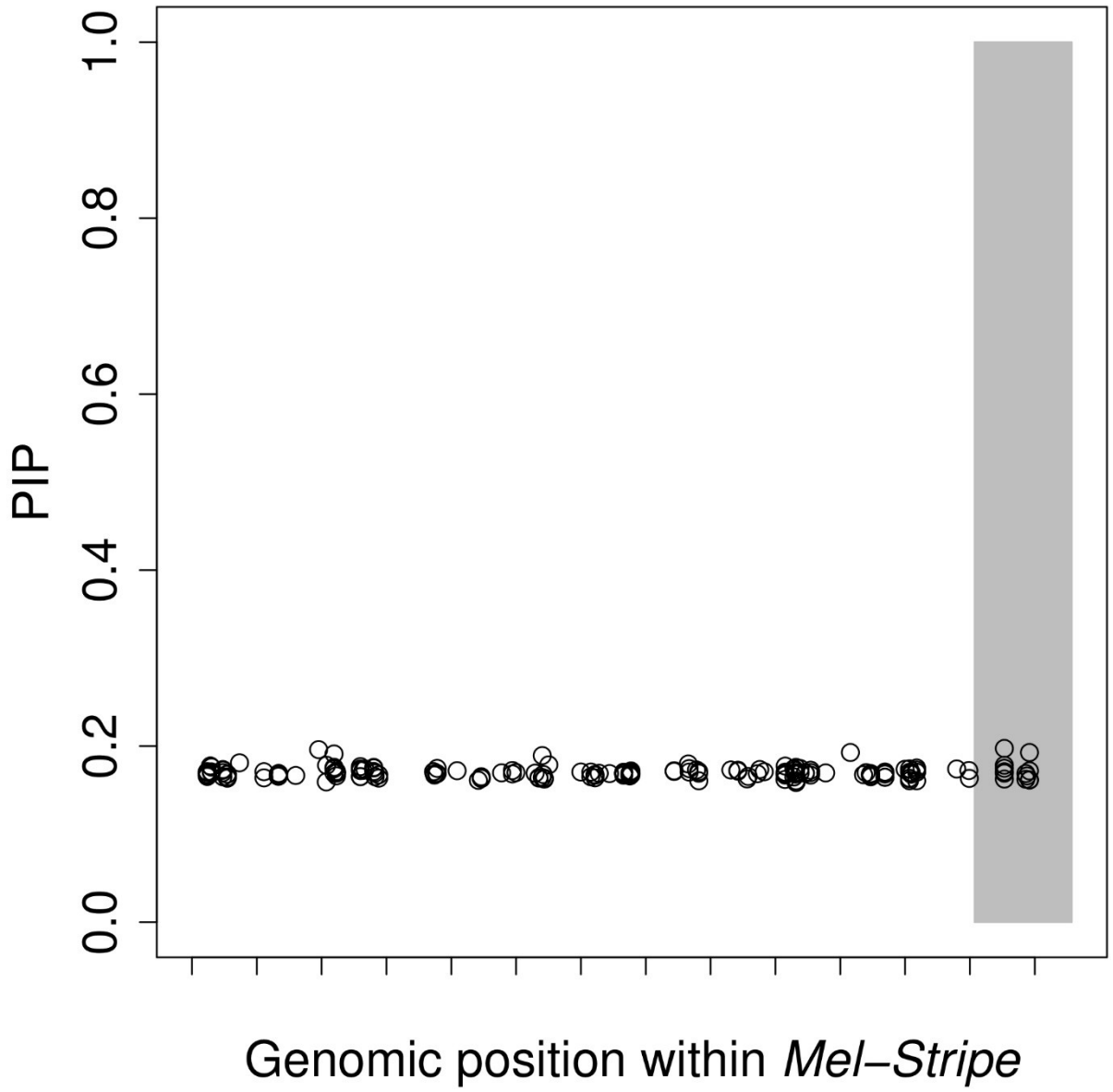

628

Figure 2. Association mapping of survival within the *Mel-Stripe* locus when epistasis is not explicitly considered. We conducted this analysis with the software GEMMA [43, 44]. The shaded grey rectangle represents the position of the indel locus within *Mel-Stripe*. The space between two ticks on the x-axis represents 1 megabase pair. PIP: posterior inclusion probability. The high PIP values of all SNPs (~0.2) is an artefact of the MCMC method and the small number of SNP tested, all SNPs within *Mel-Stripe* having some weak association with survival (see main text for further explanation).

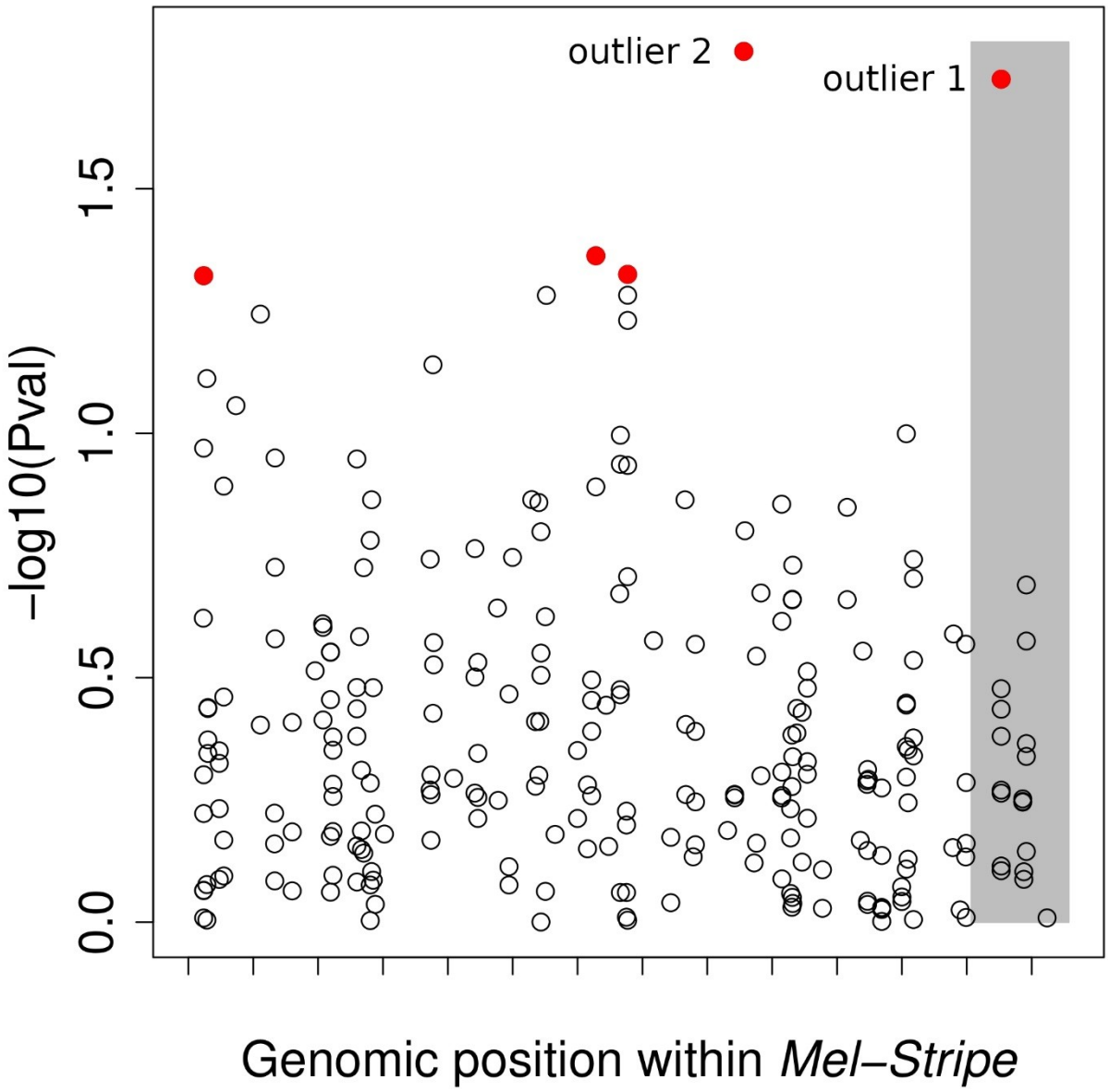

629

Figure 3. Association of survival within the *Mel-Stripe* locus, where marginal epistasis is explicitly considered. We conducted this analysis with LT-MAPIT [25, 26]. The shaded grey rectangle represents the position of the indel locus within *Mel-Stripe*. The space between two ticks on the x-axis represents 1 megabase pair. Red dots correspond to SNPs having non-zero marginal epistasis for survival with p-value <= 0.05.

630

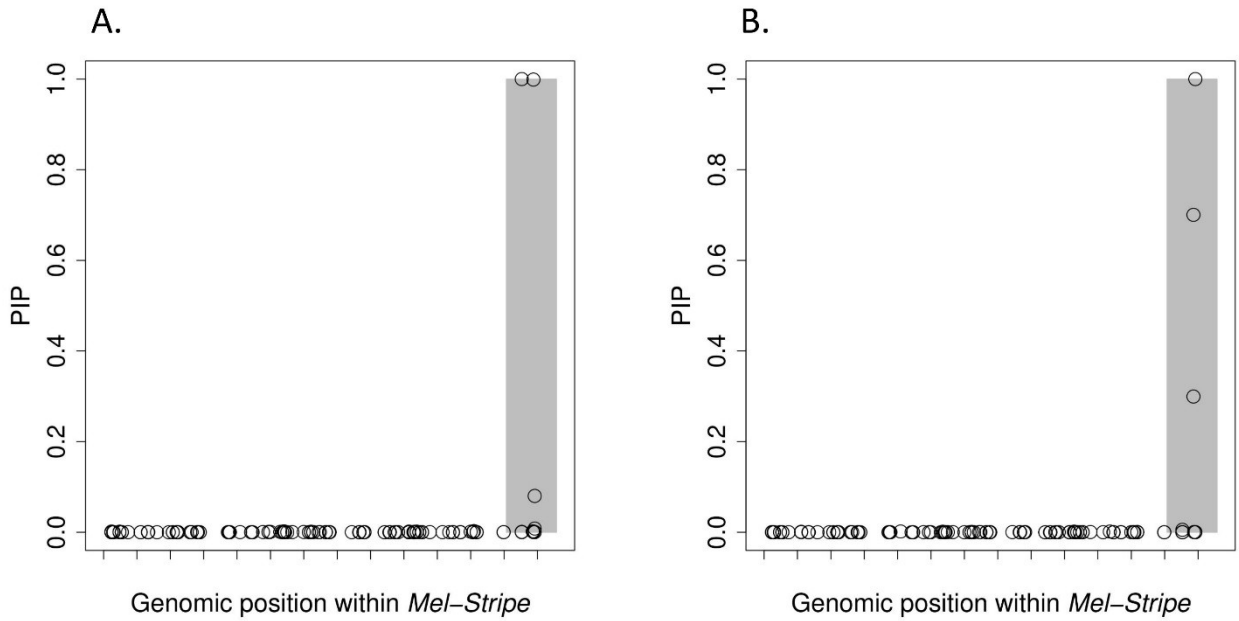

631

Figure 4. Association mapping of eye colouration within the *Mel-Stripe* locus, when epistasis is not explicitly considered. A. RG trait. B. GB trait. We conducted these analyses with GEMMA [43, 44]. The graphics display the results from the *Mel-Stripe* locus only, but because these traits are being mapped for the first time the overall analysis included genome-wide data. The shaded grey rectangle represents the position of the indel locus within *Mel-Stripe*. The space between two ticks on the x-axis represents 1 megabase pair. PIP: Posterior inclusion probability. Because of the MCMC approach, GEMMA controls for linkage disequilibrium in the results. Only SNPs explaining trait variance will be consistently retained across MCMC steps in the model.

632

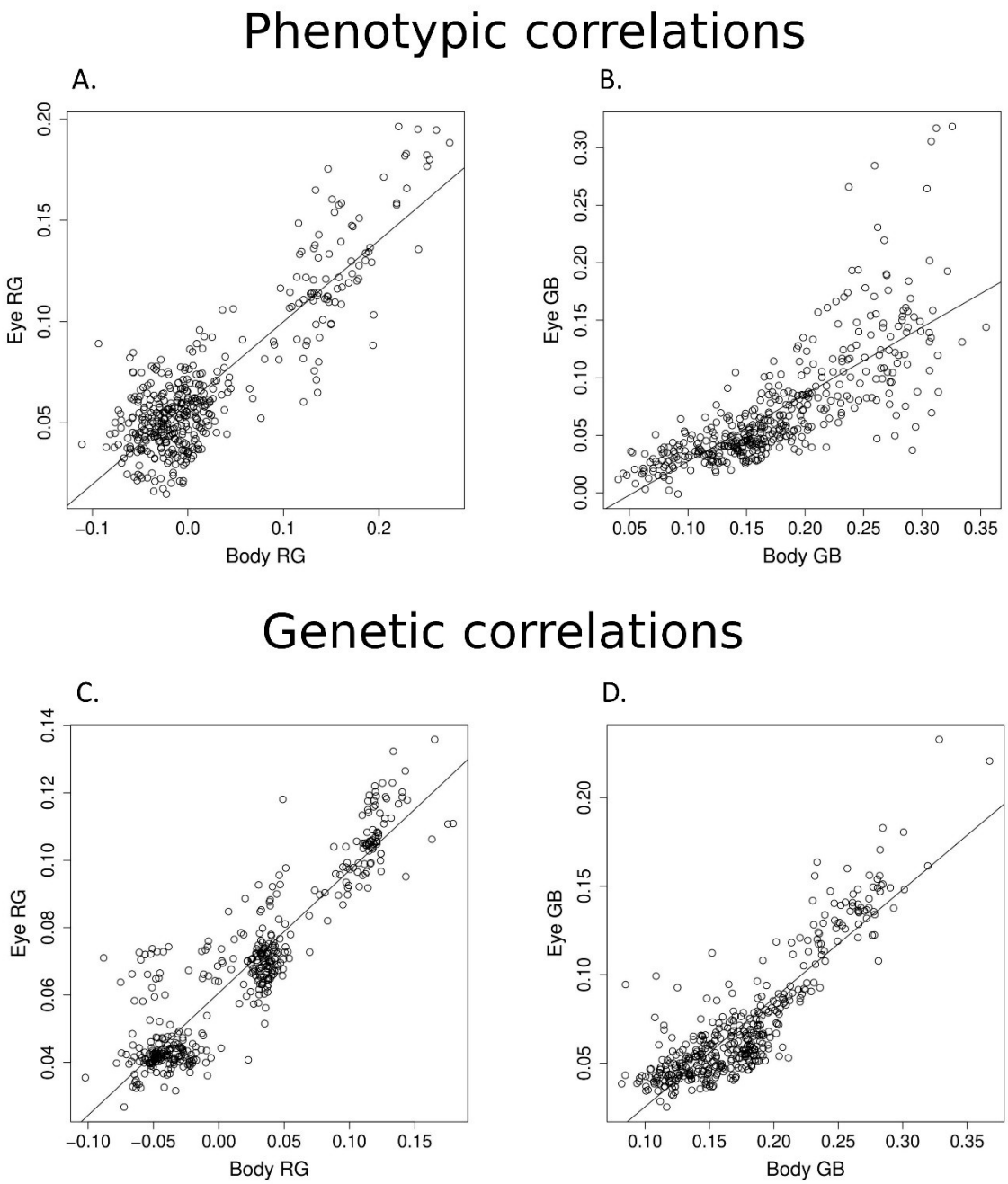

633

Figure 5. Phenotypic and genetic correlations between eye and body colouration traits (RG and GB). A&B: Phenotypic correlations. C&D: Genetic correlations, here the trait values where obtained from predictions from genotype in the software GEMMA [43, 44]. The black line represent the fit of a linear model.

References:

[1] Fisher, R. A. 1930 *The Genetical Theory of Natural Selection*, Oxford.
[2] Gillespie, J. H. 1984 Molecular Evolution Over the Mutational Landscape. *Evolution* **38**, 1116-1129. (DOI:10.2307/2408444).
[3] Orr, H. A. 2005 Theories of adaptation: what they do and don't say. *Genetica* **123**, 3-13. (DOI:10.1007/s10709-004-2702-3).
[4] Østman, B., Hintze, A. & Adami, C. 2012 Impact of epistasis and pleiotropy on evolutionary adaptation. *Proceedings of the Royal Society B: Biological Sciences* **279**, 247-256. (DOI:doi:10.1098/rspb.2011.0870).
[5] Yeaman, S. 2013 Genomic rearrangements and the evolution of clusters of locally adaptive loci. *Proceedings of the National Academy of Sciences* **110**, E1743-E1751. (DOI:10.1073/pnas.1219381110).
[6] Yeaman, S. & Symposium Editor: Michael, C. W. 2015 Local Adaptation by Alleles of Small Effect. *The American Naturalist* **186**, S74-S89. (DOI:10.1086/682405).
[7] Yeaman, S. & Whitlock, M. C. 2011 THE GENETIC ARCHITECTURE OF ADAPTATION UNDER MIGRATION–SELECTION BALANCE. *Evolution* **65**, 1897-1911. (DOI:https://doi.org/10.1111/j.1558-5646.2011.01269.x).
[8] Barrett, R. D. H., Laurent, S., Mallarino, R., Pfeifer, S. P., Xu, C. C. Y., Foll, M., Wakamatsu, K., Duke-Cohan, J. S., Jensen, J. D. & Hoekstra, H. E. 2019 Linking a mutation to survival in wild mice. *Science* **363**, 499-504. (DOI:10.1126/science.aav3824).
[9] Schluter, D., Marchinko, K. B., Arnegard, M. E., Zhang, H., Brady, S. D., Jones, F. C., Bell, M. A. & Kingsley, D. M. 2021 Fitness maps to a large-effect locus in introduced stickleback populations. *Proceedings of the National Academy of Sciences* **118**, e1914889118. (DOI:10.1073/pnas.1914889118).
[10] Méndez-Vigo, B., Picó, F. X., Ramiro, M., Martínez-Zapater, J. M. & Alonso-Blanco, C. 2011 Altitudinal and Climatic Adaptation Is Mediated by Flowering Traits and FRI, FLC, and PHYC Genes in Arabidopsis *Plant Physiol* **157**, 1942-1955. (DOI:10.1104/pp.111.183426).
[11] Zhang, L. & Jiménez-Gómez, J. M. 2020 Functional analysis of FRIGIDA using naturally occurring variation in Arabidopsis thaliana. *The Plant Journal* **103**, 154-165. (DOI:https://doi.org/10.1111/tpj.14716).
[12] Spielmann, M., Kakar, N., Tayebi, N., Leettola, C., Nürnberg, G., Sowada, N., Lupiáñez, D. G., Harabula, I., Flöttmann, R., Horn, D., et al. 2016 Exome sequencing and CRISPR/Cas genome editing identify mutations of ZAK as a cause of limb defects in humans and mice. *Genome research* **26**, 183-191. (DOI:10.1101/gr.199430.115).
[13] Adrion, J. R., Hahn, M. W. & Cooper, B. S. 2015 Revisiting classic clines in Drosophila melanogaster in the age of genomics. *Trends in genetics : TIG* **31**, 434-444. (DOI:10.1016/j.tig.2015.05.006).
[14] Cheng, C. D., Tan, J. C., Hahn, M. W. & Besansky, N. J. 2018 Systems genetic analysis of inversion polymorphisms in the malaria mosquito Anopheles gambiae. *Proceedings of the National Academy of Sciences of the United States of America* **115**, E7005-E7014. (DOI:10.1073/pnas.1806760115).
[15] Cheng, C. D., White, B. J., Kamdem, C., Mockaitis, K., Costantini, C., Hahn, M. W. & Besansky, N. J. 2012 Ecological Genomics of Anopheles gambiae Along a Latitudinal Cline: A Population-Resequencing Approach. *Genetics* **190**, 1417-1432. (DOI:10.1534/genetics.111.137794).
[16] Rennison, D. J., Heilbron, K., Barrett, R. D. H. & Schluter, D. 2015 Discriminating Selection on Lateral Plate Phenotype and Its Underlying Gene, Ectodysplasin, in Threespine Stickleback. *The American Naturalist* **185**, 150-156. (DOI:10.1086/679280).

[17] Rellstab, C., Gugerli, F., Eckert, A. J., Hancock, A. M. & Holderegger, R. 2015 A practical guide to environmental association analysis in landscape genomics. *Molecular ecology* **24**, 4348-4370. (DOI:https://doi.org/10.1111/mec.13322).
[18] Song, Z., Zhang, M., Li, F., Weng, Q., Zhou, C., Li, M., Li, J., Huang, H., Mo, X. & Gan, S. 2016 Genome scans for divergent selection in natural populations of the widespread hardwood species Eucalyptus grandis (Myrtaceae) using microsatellites. *Scientific Reports* **6**, 34941. (DOI:10.1038/srep34941).
[19] Griffiths, A. J., Miller, J. H., Suzuki, D. T., Lewontin, R. C. & Gelbart, W. M. 2000 *An Introduction to Genetic Analysis*. 7th ed. New York, USA, W. H. Freeman.
[20] Barrett, R. D. H., Rogers, S. M. & Schluter, D. 2008 Natural Selection on a Major Armor Gene in Threespine Stickleback. *Science* **322**, 255-257. (DOI:doi:10.1126/science.1159978).
[21] Michel, A. P., Sim, S., Powell, T. H. Q., Taylor, M. S., Nosil, P. & Feder, J. L. 2010 Widespread genomic divergence during sympatric speciation. *Proceedings of the National Academy of Sciences of the United States of America* **107**, 9724-9729. (DOI:10.1073/pnas.1000939107).
[22] Nosil, P., Villoutreix, R., de Carvalho, C. F., Feder, J. L., Parchman, T. L. & Gompert, Z. 2020 Ecology shapes epistasis in a genotype–phenotype–fitness map for stick insect colour. *Nature Ecology & Evolution* **4**, 1673-1684. (DOI:10.1038/s41559-020-01305-y).
[23] Wilczek, A. M., Cooper, M. D., Korves, T. M. & Schmitt, J. 2014 Lagging adaptation to warming climate in Arabidopsis thaliana. *Proceedings of the National Academy of Sciences* **111**, 7906-7913. (DOI:10.1073/pnas.1406314111).
[24] Whitlock, M. C., Phillips, P. C., Moore, F. B.-G. & Tonsor, S. J. 1995 MULTIPLE FITNESS PEAKS AND EPISTASIS. *Annual Review of Ecology and Systematics* **26**, 601-629. (DOI:10.1146/annurev.es.26.110195.003125).
[25] Crawford, L., Zeng, P., Mukherjee, S. & Zhou, X. 2017 Detecting epistasis with the marginal epistasis test in genetic mapping studies of quantitative traits. *PLoS genetics* **13**, e1006869. (DOI:10.1371/journal.pgen.1006869).
[26] Crawford, L. & Zhou, X. 2018 Genome-wide marginal epistatic association mapping in case-control studies. *bioRxiv*.
[27] Comeault, A. A., Flaxman, S. M., Riesch, R., Curran, E., Soria-Carrasco, V., Gompert, Z., Farkas, T. E., Muschick, M., Parchman, T. L., Schwander, T., et al. 2015 Selection on a Genetic Polymorphism Counteracts Ecological Speciation in a Stick Insect. *Curr Biol* **25**, 1975-1981. (DOI:10.1016/j.cub.2015.05.058).
[28] Sandoval, C. P. 1994 Differential visual predation on morphs of Timema cristinae (Phasmatodeae:Timemidae) and its consequences for host range. *Biol J Linn Soc* **52**, 341-356. (DOI:doi:10.1111/j.1095-8312.1994.tb00996.x).
[29] Villoutreix, R., de Carvalho, C. F., Soria-Carrasco, V., Lindtke, D., De-la-Mora, M., Muschick, M., Feder, J. L., Parchman, T. L., Gompert, Z. & Nosil, P. 2020 Large-scale mutation in the evolution of a gene complex for cryptic coloration. *Science* **369**, 460-466. (DOI:10.1126/science.aaz4351).
[30] Villoutreix, R., Ayala, D., Joron, M., Gompert, Z., Feder, J. L. & Nosil, P. 2021 Inversion breakpoints and the evolution of supergenes. *Molecular ecology* **30**, 2738-2755. (DOI:https://doi.org/10.1111/mec.15907).
[31] Dobzhansky, T. G. 1947 Adaptive Changes Induced by Natural Selection in Wild Populations of Drosophila. *Evolution* **1**, 1-16. (DOI:10.2307/2405399).
[32] Kirkpatrick, M. 2010 How and Why Chromosome Inversions Evolve. *Plos Biol* **8**, e1000501. (DOI:10.1371/journal.pbio.1000501).
[33] Darlington, C. D. & Mather, K. 1949 *The elements of Genetics*. London, George Allen & Unwind LTD.
[34] Gu, X., Li, Z., Su, Y., Zhao, Y. & Liu, L. 2019 Imaginal disc growth factor 4 regulates development and temperature adaptation in Bactrocera dorsalis. *Scientific Reports* **9**, 931. (DOI:10.1038/s41598-018-37414-9).

[35] Lu, X.-Y., Li, J., Liu, X., Li, X. & Ma, J. 2014 Characterization and expression analysis of six chitinase genes from the desert beetle Microdera punctipennis in response to low temperature. *Cryo letters* **35 5**, 438-448.
[36] Francikowski, J., Krzyżowski, M., Kochańska, B., Potrzebska, M., Baran, B., Chajec, Ł., Urbisz, A., Małota, K., Łozowski, B., Kloc, M., et al. 2019 Characterisation of white and yellow eye colour mutant strains of house cricket, Acheta domesticus. *PloS one* **14**, e0216281-e0216281. (DOI:10.1371/journal.pone.0216281).
[37] Larkin, A., Marygold, S. J., Antonazzo, G., Attrill, H., dos Santos, G., Garapati, P. V., Goodman, Joshua L., Gramates, L S., Millburn, G., Strelets, V. B., et al. 2020 FlyBase: updates to the Drosophila melanogaster knowledge base. *Nucleic Acids Research* **49**, D899-D907. (DOI:10.1093/nar/gkaa1026).
[38] Liu, G., Liu, W., Zhao, R., He, J., Dong, Z., Chen, L., Wan, W., Chang, Z., Wang, W. & Li, X. 2021 Genome-wide identification and gene-editing of pigment transporter genes in the swallowtail butterfly Papilio xuthus. *BMC Genomics* **22**, 120. (DOI:10.1186/s12864-021-07400-z).
[39] Vargas-Lowman, A., Armisen, D., Burguez Floriano, C. F., da Rocha Silva Cordeiro, I., Viala, S., Bouchet, M., Bernard, M., Le Bouquin, A., Santos, M. E., Berlioz-Barbier, A., et al. 2019 Cooption of the pteridine biosynthesis pathway underlies the diversification of embryonic colors in water striders. *Proceedings of the National Academy of Sciences* **116**, 19046-19054. (DOI:10.1073/pnas.1908316116).
[40] Gompert, Z., Comeault, A. A., Farkas, T. E., Feder, J. L., Parchman, T. L., Buerkle, C. A. & Nosil, P. 2014 Experimental evidence for ecological selection on genome variation in the wild. *Ecology Letters* **17**, 369-379. (DOI:https://doi.org/10.1111/ele.12238).
[41] Nosil, P. & Crespi, B. J. 2006 Experimental evidence that predation promotes divergence in adaptive radiation. *Proceedings of the National Academy of Sciences of the United States of America* **103**, 9090-9095. (DOI:10.1073/pnas.0601575103).
[42] PARCHMAN, T. L., GOMPERT, Z., MUDGE, J., SCHILKEY, F. D., BENKMAN, C. W. & BUERKLE, C. A. 2012 Genome-wide association genetics of an adaptive trait in lodgepole pine. *Molecular ecology* **21**, 2991-3005. (DOI:https://doi.org/10.1111/j.1365-294X.2012.05513.x).
[43] Zhou, X., Carbonetto, P. & Stephens, M. 2013 Polygenic Modeling with Bayesian Sparse Linear Mixed Models. *PLoS genetics* **9**, e1003264. (DOI:10.1371/journal.pgen.1003264).
[44] Zhou, X. & Stephens, M. 2012 Genome-wide efficient mixed-model analysis for association studies. *Nature Genetics* **44**, 821-824. (DOI:10.1038/ng.2310).
[45] Altschul, S. F., Gish, W., Miller, W., Myers, E. W. & Lipman, D. J. 1990 Basic local alignment search tool. *Journal of Molecular Biology* **215**, 403-410. (DOI:https://doi.org/10.1016/S0022-2836(05)80360-2).
[46] Nosil, P., Villoutreix, R., de Carvalho, C. F., Farkas, T. E., Soria-Carrasco, V., Feder, J. L., Crespi, B. J. & Gompert, Z. 2018 Natural selection and the predictability of evolution in Timema stick insects. *Science* **359**, 765-770. (DOI:10.1126/science.aap9125).
[47] Schneider, C. A., Rasband, W. S. & Eliceiri, K. W. 2012 NIH Image to ImageJ: 25 years of image analysis. *Nat Methods* **9**, 671-675. (DOI:10.1038/nmeth.2089).
[48] Endler, J. A. 2012 A framework for analysing colour pattern geometry: adjacent colours. *Biol J Linn Soc* **107**, 233-253. (DOI:10.1111/j.1095-8312.2012.01937.x).
[49] Raftery, A. E. 1995 Bayesian Model Selection in Social Research. *Sociological Methodology* **25**, 111-163. (DOI:10.2307/271063).
[50] Team, R. C. 2020 R: A language and environment for statistical computing. *R Foundation for Statistical Computing, Vienna, Austria.* (DOI:URL https://www.R-project.org/).
[51] Chapman, R. F. 2012 *The Insects: Structure and Function*. Fifth edition ed. Cambridge, UK, Cambridge university Press.
[52] Tearle, R. G., Belote, J. M., McKeown, M., Baker, B. S. & Howells, A. J. 1989 Cloning and characterization of the scarlet gene of Drosophila melanogaster. *Genetics* **122**, 595-606.

[53] Zhao, J. T., Bennett, C. L., Stewart, G. J., Frommer, M. & Raphael, K. A. 2003 The scarlet eye colour gene of the tephritid fruit fly: Bactrocera tryoni and the nature of two eye colour mutations. *Insect Molecular Biology* **12**, 263-269. (DOI:https://doi.org/10.1046/j.1365-2583.2003.00410.x).
[54] Okude, G. & Futahashi, R. 2021 Pigmentation and color pattern diversity in Odonata. *Current Opinion in Genetics & Development* **69**, 14-20. (DOI:https://doi.org/10.1016/j.gde.2020.12.014).
[55] Concha, C., Wallbank, R. W. R., Hanly, J. J., Fenner, J., Livraghi, L., Rivera, E. S., Paulo, D. F., Arias, C., Vargas, M., Sanjeev, M., et al. 2019 Interplay between Developmental Flexibility and Determinism in the Evolution of Mimetic Heliconius Wing Patterns. *Curr Biol* **29**, 3996-4009.e3994. (DOI:https://doi.org/10.1016/j.cub.2019.10.010).
[56] Archambeault, S. L., Bärtschi, L. R., Merminod, A. D. & Peichel, C. L. 2020 Adaptation via pleiotropy and linkage: Association mapping reveals a complex genetic architecture within the stickleback Eda locus. *Evolution Letters* **4**, 282-301. (DOI:https://doi.org/10.1002/evl3.175).
[57] Ford, E. B. 1965 *Genetic Polymorphism*. London, Studies Faber & Faber.
[58] Ford, E. B. 1971 *Ecological Genomics*. 3rd ed. London, Chapman and Hall LTD.
[59] Lindtke, D., Lucek, K., Soria-Carrasco, V., Villoutreix, R., Farkas, T. E., Riesch, R., Dennis, S. R., Gompert, Z. & Nosil, P. 2017 Long-term balancing selection on chromosomal variants associated with crypsis in a stick insect. *Molecular ecology* **26**, 6189-6205. (DOI:10.1111/mec.14280).
[60] Navarro, A. & Barton, N. H. 2003 Chromosomal Speciation and Molecular Divergence--Accelerated Evolution in Rearranged Chromosomes. *Science* **300**, 321-324. (DOI:10.1126/science.1080600).
[61] Kirkpatrick, M. & Barton, N. 2006 Chromosome Inversions, Local Adaptation and Speciation. *Genetics* **173**, 419-434. (DOI:10.1534/genetics.105.047985).
[62] Feder, J. L., Gejji, R., Powell, T. H. Q. & Nosil, P. 2011 ADAPTIVE CHROMOSOMAL DIVERGENCE DRIVEN BY MIXED GEOGRAPHIC MODE OF EVOLUTION. *Evolution* **65**, 2157-2170. (DOI:10.1111/j.1558-5646.2011.01321.x).